www.czasopisma.pan.pl PAN www.journals.pan.pl
Opto-Electronics Review 26 (2018) 24–28

Contents lists available at ScienceDirect

Opto-Electronics Review

journal homepage: http://www.journals.elsevier.com/opto-electronics review

# Dual-resonance long-period grating in fiber loop mirror structure for liquid refractive index measurement

R. Zawisza [a,b,*], T. Eftimov [b], P. Mikulic [b], Y. Chinifooroshan [b], A. Celebańska [b], W.J. Bock [b], L.R. Jaroszewicz [a]

[a] Institute of Applied Physics, Faculty of Advanced Technologies and Chemistry, Military University of Technology, 2 gen. Sylwestra Kaliskiego St., Warsaw, 00-908, Poland
[b] Photonics Research Center, Université du Québec en Outaouais, 101 Rue St Jean Bosco, Pavillon Lucien Brault, Gatineau, Québec, J8X 3X7, Canada

ARTICLE INFO

*Article history:*
Received 19 September 2017
Received in revised form
20 November 2017
Accepted 23 November 2017
Available online 14 December 2017

*Keywords:*
Optical engineering
Polarization-maintaining fiber
Dual-resonance long-period grating
Fiber optics sensors
Fiber loop mirror

ABSTRACT

An interferometric structure based on a Dual-Resonance Long-Period Grating (DRLPG) within a Fiber Loop Mirror (FLM) is presented in this paper. Its purpose is to measure the refractive index (RI) of liquid analytes. The grating is the RI sensing probe, while the FLM serves as a band-pass filter. Due to the high extinction ratio of the FLM, amplitude measurements can be obtained, allowing implementation of the differential interrogation method to establish the sensitivity of the device. The use of a polarization controller makes it possible to fine-tune the interferometric peaks with respect to the two notches of the DRLPG. Precisely aligned configuration produces a maximum sensitivity of 3871.5 dB/RIU within the RI range of 1.3333 up to 1.3419 with linear sensor response.



## 1. Introduction

Long Period Gratings (LPGs) have become very popular as platforms for chemical [1], biological [2] and physical [3,4] sensors because of their low cost, compact size and insensitivity to ambient electro-magnetic fields [5]. In recent years, different fiber configurations based on LPGs for liquid refractive index (RI) detection have been described [6], which were characterized by a very high sensitivity to resonant dip shifts caused by changes in the surrounding refractive index (SRI) [7]. This excellent sensitivity of LPGs is achieved by coupling of a guided fundamental mode to higher order cladding mode. This phenomenon leads to the appearance of two resonance peaks created by the transfer of energy to the same cladding mode at two discrete wavelengths [8]. In other words, there are two modes with identical group velocities in the LPG under conditions that lead to a broadband mode conversion [9]. When the sensing probe is exposed to an ambient perturbation, the phase matching condition changes. For this reason, the two resonant notches of the LPG shift in opposite directions [10] and thus, the sensor can work close to the turning point of the dispersion curve [11], where the sensitivity is ultrahigh [12].

RI sensors in interferometric configuration have been widely described, where the RI sensitivity part has been obtained by modification of polarization maintaining (PM) fiber. Zhong et al. [13] proposed a refractometer formed by insertion of two sections of PM fiber with different lengths, with one of the PM fibers chemically etched and used as a sensing part. Wang et al. [14] presented a compact structure of an in-line Mach-Zehnder interferometer made by femtosecond laser micromachining that achieved sensitivity of 9370 nm/RIU within the RI range between 1.31 and 1.335. Modulation in the resonant condition causes spectral shifts of both LPG notches. Since the dual-resonance long period grating (DRLPG) has a very low extinction ratio, the sensitivity response cannot be expressed by a true-amplitude modulation. Chu et al. [15] present the design of a sensor for RI measurement using a high-birefringence fiber loop mirror (HB-FLM) concatenated with the LPG. A major goal in that paper was measurement of the intensity demodulation by simple use of an optical power meter (OPM). The authors achieved a maximum LPG sensitivity level expressed in transmission intensity of 103.2 dB/RIU.

In this paper, for the first time to authors knowledge, a new approach to liquid RI sensor based on a DRLPG inside a FLM compared to previously proposed [16–18], in which the sensitivity level is expressed by the intensity is presented. Paper demonstrates that

* Corresponding author at: Photonics Research Center, Université du Québec en Outaouais, 101 Rue St Jean Bosco, Pavillon Lucien Brault, Gatineau, Québec, J8X 3X7, Canada.
*E-mail address:* renata.wonko@wat.edu.pl (R. Zawisza).

https://doi.org/10.1016/j.opelre.2017.11.002
1230-3402/

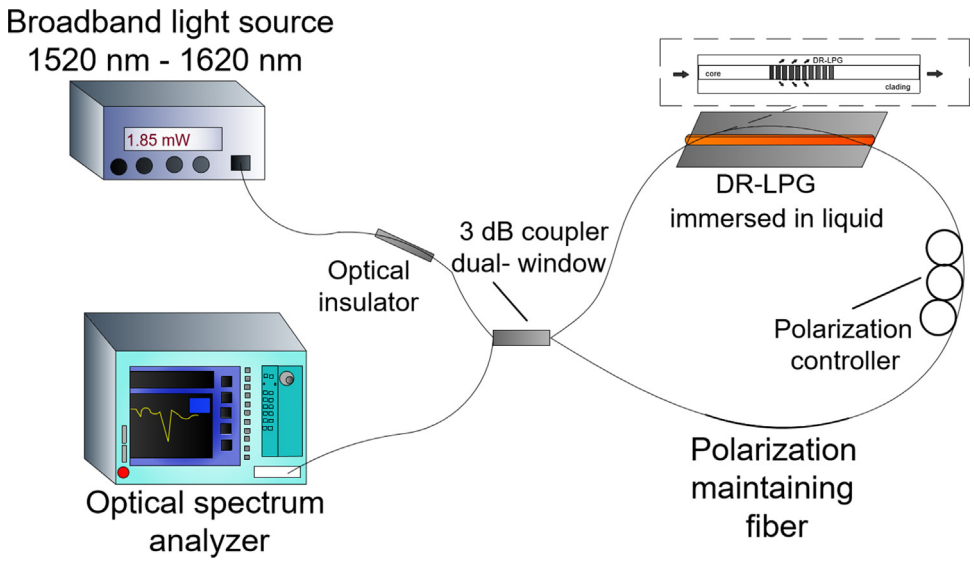


**Fig. 1.** Experimental set-up of the DRLPG inside an FLM for accurate liquid refractive index measurement.

the inherent state of polarization of the propagating beam enables adjustment of peaks which come from the FLM and the DRLPG. Placing the DRLPG inside the FLM makes it possible to implement a differential interrogation method with a sensitivity of an order of magnitude higher than in other configurations. The combination of these two optical components overcome limitations related to the low extinction ratio of the DRLPG, so that the grating acts as a broadband true-amplitude modulator of the refractometer. These two discrete properties underpin the design of the device proposed here, the FLM-DRLPG, whose amplitude of peaks is changed for an arbitrary small variation of the ambient refractive index (ARI).

## 2. Theory and experimental set-up

The main relation describing resonance wavelength coupling of the guided core mode and the m$^{th}$ cladding mode in an LPG is given as [19]:

$$\lambda_{eff}^{m} = \left(n_{eff}^{0,1} - n_{eff}^{0,m}\right) \cdot \Lambda \tag{1}$$

where, $n_{eff}^{0,1}$ is the effective RI of the propagating fundamental mode, $n_{eff}^{0,m}$ is the effective RI of the m$^{th}$ cladding mode and $\Lambda$ is the grating period.

The scheme of the proposed FLM-DRLPG configuration is presented in Fig. 1. The FLM consists of a wideband 3 dB coupler, a section of a PM fiber – Fibercore HB 1500 (bow-tie type) – and a polarization controller (PC). A DRLPG was placed after the 3 dB coupler but before the PC. The FLM was illuminated by a broadband light source with a spectral bandwidth range from 1520 nm up to 1620 nm. An optical insulator was used to protect the optical devices against the potential instability of the propagating light. The 3 dB coupler splits the input light into two optical beams which counter-propagate around the loop and through the DRLPG, the PM and the PC. The two beams propagate with different velocities, which means that their individual state of polarization varies and the two beams interfere in the output [20]. The obtained interference pattern was monitored by an optical spectrum analyzer (OSA) with a resolution of 0.1 nm. Taking into account the operating wavelength range of the tested grating and PM fiber, the OSA spectra range was from 1520 nm to 1620 nm. However, in a future application, the OSA could be replaced by an OPM, provided the transmission spectrum of the FLM-DRLPG was fine-tuned and appropriately filtered. Hence, comparing proposed FLM-DRLPG sensor structure with sensor based on only LPG or DRLPG, the FLM-DRLPG is less expensive due to the possibility of replacement of an optical spectrum analyzer by the simple power meter, which is much cheaper.

In this experiment the DRLPG was made by an amplitude mask technique using a high-power KrF Excimer laser (Lumonics$^{TM}$ Lasers: Pulse Master $^{®}$-840) emitting at 248 nm [21]. A section of bare fiber (Corning SMF28) was exposed to UV radiation through a chromium amplitude mask with a pitch of $\Lambda = 217\,\mu m$, which ensured coupling of the fundamental mode to a mode higher than the $LP_{0,11}$ cladding mode. Excitation of a double resonance was thus achieved. The peak pulse energy of the excimer laser was 340 nJ. After this, the LPG was annealed at a temperature of 150 °C for 90 minutes in order to release the excess hydrogen. The transmission spectra of the DRLPG was optimized by reducing the cladding diameter through partial etching with 10% Hydrofluoric acid (HF 10%) [22].

In order to match the fringe pattern to the notches of the DRLPG, the length of the PM fiber must be accurately determined. Knowing the distance between notches of the DRLPG, which was 17 nm, and taking into account the birefringence value of the PM fiber as well as the central operating wavelength of the sensor (1550 nm), the length L of PM fiber from the formula [23] is calculated as:

$$L = \frac{\lambda^2}{B\Lambda_\lambda} \tag{2}$$

where B, $\Lambda_\lambda$ and $\lambda$ are respectively the group modal birefringence of the PM fiber, the distance between notches and the operating wavelength.

The computed length of the PM fiber was 0.31 m. Fig. 2 shows the transmission spectra of the tuned FLM-DRLPG structure so that both notches of the resonance peaks are exactly covered by interference dips.

The PC was inserted between the DRLPG and the section of PM fiber to tune the transmission spectra of the FLM. This possibility was mentioned in Ref. [13], although the authors of that work provided no details. The interference peaks could be moved up to 9 nm by changing the state of polarization (SOP) of the propagating beam as well as the amplitude for about 11.25 dBm (Fig. 3).

Since the dual resonance of the LPG is visible on the transmission spectra within the specified ARI, the interference peaks have to be adjusted for the appropriate sensor range. In other words, the interference peaks should be tuned right before both notches of

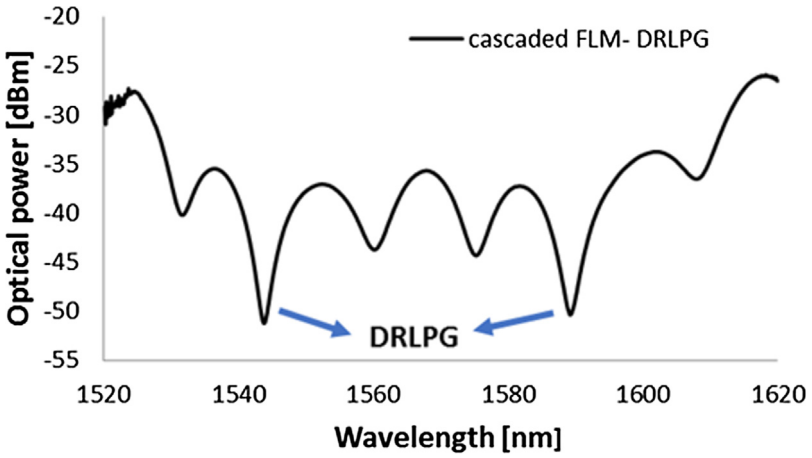


**Fig. 2.** Transmission spectrum of the FLM-DRLPG structure (pitch $\Lambda = 217\ \mu m$), when the LPG was immersed in water. The state of polarization was set up to highlight the resonant peaks.

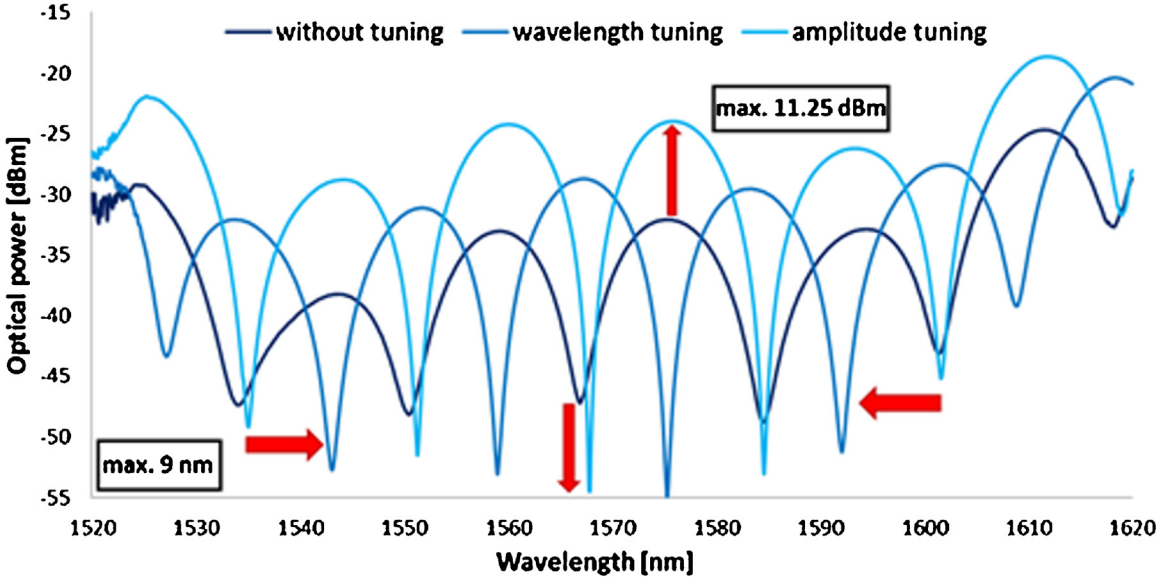


**Fig. 3.** Transmission spectra of the FLM-DRLPG without tuning (black line), with wavelength tuning (dark blue line) and with amplitude tuning (light blue line).

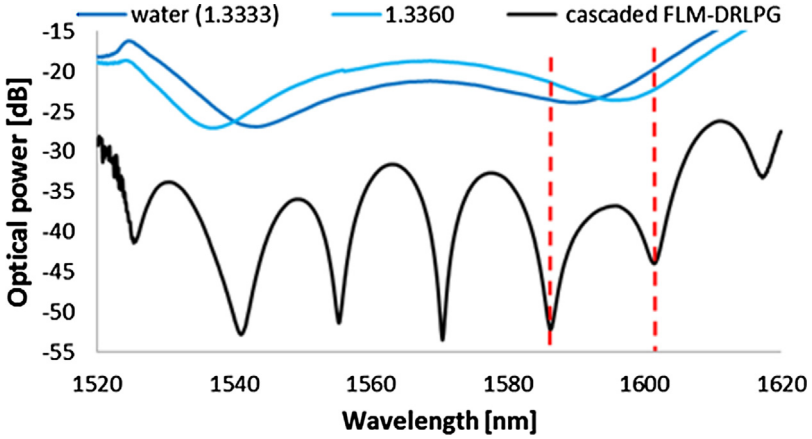


**Fig. 4.** Transmission spectra of the DRLPG immersed in water RI = 1.3333 (dark blue) and in dilution of deionized water and glycerin RI=1.3360 (light blue). The transmission spectrum of the tuned FLM-DRLPG structure immersed in water is marked by the black line. The red dashed line indicates the points of FLM adjustment.

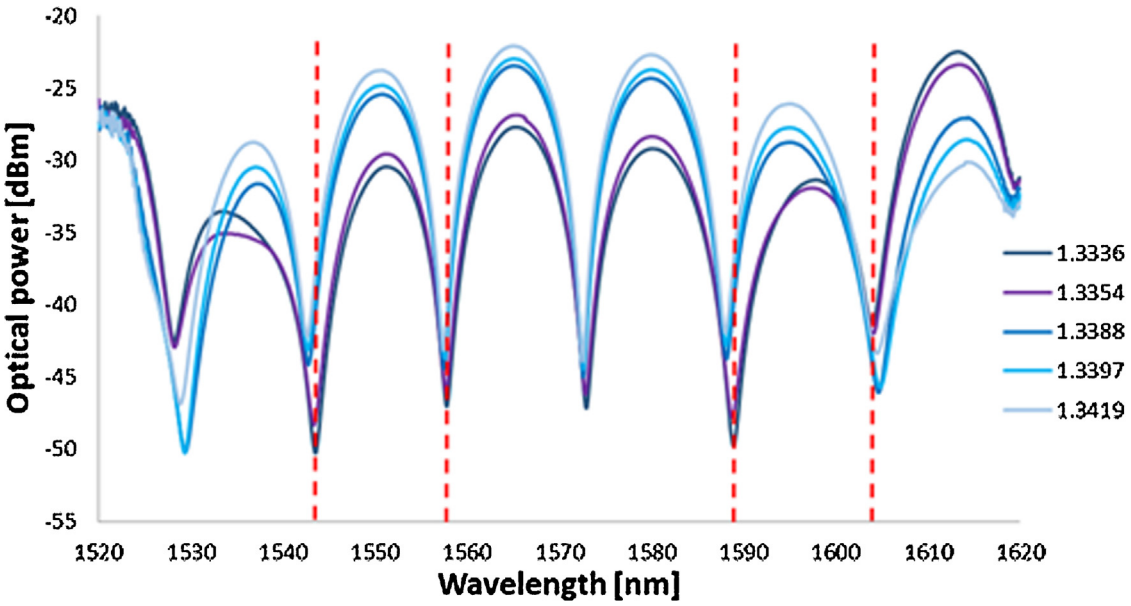


**Fig. 5.** Transmission spectra of the sensor for different ARI values. Red dashed lines mark the points used for calculation.

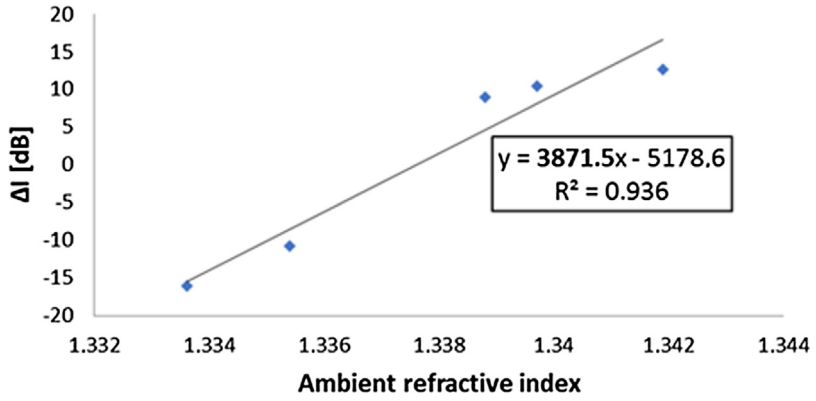


**Fig. 6.** Sensor response to the liquid refractive index variation. Sensitivity is expressed in intensity changes and is calculated using the differential signal interrogation method.

the DRLPG for the RI of water and right after both notches for the highest value of the ARI of the sensor (red dashed lines in Fig. 4).

The DRLPG acts as the sensor head, while the FLM functions as a band-pass filter. For the liquid RI sensitivity measurements, the DRLPG was placed inside a U-groove, which was attached to the XYZ translational stage. The 3-axis positioning of the translation U-groove provides centric placement of the DRLPG inside the measured liquid. This ensures the same thickness of liquid samples around the DRLPG so that only RI changes have an influence on boundary conditions. The grating was clamped on one side and loaded on the other side. Hence, each measurement was conducted with the same stress on the DRLPG and measurement errors were reduced to the minimum. Moreover, each measurement was carried out in the same temperature, guaranteeing that the influence of temperature on the transmission spectrum change was negligible.

## 3. Results and discussion

To provide exact RI measurements, liquid dilutions were made by mixing accurate concentrations of deionized water with glycerin to achieve liquid samples with RI values in the range from 1.3333 to 1.3419. Each successive measurement required precise cleaning of the DRLPG surface. Liquid samples were characterized by Abbe refractometer before and after each test. If any difference was found, the measurement for that particular ARI value was repeated.

Fig. 5 shows the transmission spectra of the FLM-DRLPG structure for different ARI values. When the liquid's RI increases, the amplitude of the interference dips changes in coverage area by both notches of the DRLPG. The rest of the FLM peaks remain intact, although they are encumbered with an error caused by the wavelength shift, which was estimated at ±0.3 nm. It should also be mentioned that some dips shift towards longer wavelengths, while others shift in the opposite direction. This is due to the dispersive nature of the DRLPG. Since the depths of the two LPG notches are different, the amplitude of interference peaks varies unevenly with the ARI change. As a result, the difference between interference dips associated with the LPG notches can express greater than normal changes with external variation of the ARI.

The unique properties of the DRLPG response to ARI made it possible to apply a specific calculation of the sensitivity. The intensity of the four dips (marked by red dashed lines in Fig. 5) was monitored by recording the intensity changes at discrete wavelengths with respect to the initial peak adjustment. Because the interference peaks act as a band-pass filter, the differential signal interrogation method could be applied. This method is based on the measurement of the difference between a constant and a variable

value with the same physical quantity. First, the two adjacent interference peaks for the first and the second notches of the DRLPG (see the red dashed lines in Fig. 5) were chosen. Second, the difference between the intensities on the either side of each notch was calculated. Last, the difference between the results for the two notches was computed. The result expresses the enhanced sensitivity of the liquid RI sensor in terms of the intensity (in dB).

In these tests, a range of approximately 30 dB for ARI changes from 1.3336 to 1.3419 was obtained. As shown in Fig. 6, there is a good linear relationship between the liquid ARI and the difference in the intensities of the interference dips with a relative coefficient reaching 0.936. Unfortunately as one can see there is a relatively high scattering of measuring points. Because the sensor response is measured as a amplitude change (not as a wavelength shift) the peaks which comes from interference and resonance should be overlap in appropriate way. In this case, as it seen in Fig. 5 (wavelength between 1530–1540 nm), the amplitude varies. To resolve this problem, in the future, the another DRLPG will be adopted, with bigger distance between both LPG notches. The maximum sensitivity recorded was 3871.5 dB/RIU for the tested range. Moreover, the symmetry of the sensor response is due to the opposite displacement of the DRLPG notches.

## 4. Conclusions

Any report about a sensor based on the FLM-DRLPG structure which can make a direct comparison has not been found. However, in one previously reported configuration [14], an FLM was used with a standard LPG and that configuration showed one order of magnitude lower sensitivity than demonstrated in this paper. The monitoring of the amplitude changes enabled us to apply a differential interrogation method to obtain a signal expressed in dB as a computational tool for sensitivity enhancement. The FLM was chosen in this configuration because in contrast to a traditional interferometer, it is independent of the input polarization state since one beam propagates clockwise and the other propagates counter-clockwise along the same optical path. This means that the reference signal and the signal under test are the same and thus there is no need to align the optical paths. They are also exposed to the same environmental conditions so that ambient disturbances are not an issue. Combining the unique properties of a DRLPG and the interferometric function of an FLM and adding the possibility of tuning attenuation dips by adjusting the SOP a high amplitude sensitivity optical fiber refractometer has been produced. This device is expected to operate in ARI variation mode with detection provided by a simple OPM. Due to the fact, that both FLM and DRLPG are sensitive to the temperature, further researches on the FLM-DRLPG sensor for distinguish RI and temperature response are in progress. In this case, the cross-sensitivity can be eliminated because sensor in such optics configuration is dual-parameter sensor, which has opposite response for RI and temperature measurement.

## Acknowledgements

This work was supported by the Natural Sciences and Engineering Research Council of Canada for the SPI/NSERC Industrial Research Chair in Photonic Sensing Systems for Safety and Security Monitoring. Our investigation was also partially supported by the internal Military University of Technology project no. RMN 08/690.

## References

[1] S.W. James, S. Korposh, S. Lee, R.P. Tatam, A long period grating-based chemical sensor insensitive to the influence of interfering parameters, Opt. Express 22 (7) (2014) 8012–8023.
[2] X. Chen, L. Zhang, K. Zhou, E. Davies, K. Sugden, I. Bennion, M. Hughes, A. Hine, Real-time detection of DNA interactions with long-period fiber-grating-based biosensor, Opt. Lett. 32 (17) (2007) 2541–2543.
[3] Q. Liu, K.S. Chiang, K.P. Lor, Condition for the realization of a temperature-insensitive long-period waveguide grating, Opt. Lett. 31 (18) (2006) 2716–2718.
[4] X. Zhong, Y. Wang, J. Qu, Ch. Liao, Sh. Liu, J. Tang, Q. Wang, J. Zhao, K. Yang, Zh. Li, High-sensitivity strain sensor based on inflated long period fiber grating, Opt. Lett. 39 (18) (2014) 5463–5466.
[5] B. Culshaw, Fiber optics in sensing and measurement, IEEE J. Sel. Top. Quantum Electron. 6 (6) (2000) 1014–1021.
[6] V. Grubsky, J. Feinberg, Long-period fiber gratings with variable coupling for real-time sensing applications, Opt. Lett. 25 (4) (2000) 203–205.
[7] P.K. Sahoo, J. Joseph, R. Yukino, A. Sandhu, High sensitivity refractive index sensor based on simple diffraction from phase grating, Opt. Lett. 41 (9) (2016) 2101–2104.
[8] X. Shu, S. Zhu, Q. Wang, S. Jiang, W. Shi, Z. Huang, E. Huang, Dual resonant peaks of LP015 cladding mode in long-period gratings, Electron. Lett. 35 (18) (1999) 649–651.
[9] S. Ramachandran, S. Ghalmi, Zh. Wang, M. Yan, Band-selection filters with concatenated long-period gratings, Opt. Lett. 27 (19) (2002) 1678–1680.
[10] S.M. Tripathi, E. Marin, A. Kumar, J. Meunie, Bragg grating based biochemical sensor using submicron Si/SiO2Si/SiO2 waveguides for lab-on-a-chip applications: a novel design, App. Opt. 48 (31) (2009) 4562–4567.
[11] X. Shu, L. Zhang, I. Bennion, Sensitivity characteristics of long-period fiber gratings, J. Lightwave Technol. 20 (2) (2002) 255–266.
[12] Zh. Wang, S. Ramachandran, Ultrasensitive long-period fiber gratings for broadband modulators and sensors, Opt. Lett. 28 (24) (2003) 2458–2460.
[13] Ch. Zhong, Ch. Shen, Y. You, J. Chu, X. Zou, X. Dong, Y. Jin, J. Wang, A polarization-maintaining fiber loop mirror based sensor for liquid refractive index absolute measurement, Sens. Actuators B: Chem. 168 (2012) 360–364.
[14] Y. Wang, M. Yang, D.N. Wang, Sh. Liu, P. Lu, Fiber in-line Mach–Zehnder interferometer fabricated by femtosecond laser micromachining for refractive index measurement with high sensitivity, J. Opt. Soc. Am. B 27 (3) (2010) 370–374.
[15] J. Chu, Ch. Shen, Ch. Zhong, X. Zou, K. Li, X. Dong, Long-period fiber grating based cantilever strain, in: In Proceedings of the 2012 Symposium on Photonics and Optoelectronics (SOPO), Shanghai, China, 21–23 May, 2012, pp. 1–3.
[16] J. Chu, Ch. Shen, F. Quian, Ch. Zhong, X. Zou, X. Dong, Y. Jin, J. Wang, Y. Gong, T. Jiang, Simultaneous measurement of strain and temperature based on a long-period grating with a polarization maintaining fiber in a loop mirror, Opt. Fiber Technol. 20 (1) (2014) 44–47.
[17] J. Wang, Ch. Shen, Y. Lu, D. Chen, Ch. Zhong, J. Chu, X. Dong, C.C. Chan, Liquid refractive index sensor based on a polarization-maintaining fiber loop mirror, IEEE Sens. J. 13 (5) (2012) 1721–1724.
[18] T. Hu, Y. Zhao, L. Cai, Temperature and refractive index sensor using a high-birefringence fiber loop mirror and single mode-coreless-single mode fiber structure, Instrum. Sci. Technol. 44 (4) (2015) 366–376.
[19] X. Shu, L. Zhang, I. Bennion, Sensitivity characteristics of long-period fiber gratings, J. Lightwave Technol. 20 (2) (2002) 255–266.
[20] O. Frazão, J.M. Baptisa, J.L. Santos, REcent advances in high-birefringence fiber loop mirror sensors, Sensors 7 (2007) 2970–2983.
[21] R.Y.N. Wong, E. Chehura, S.E. Staines, S.W. James, R.P. Tatam, Fabrication of fiber optic long period gratings operating at the phase matching turning point using an ultraviolet laser, Appl. Opt. 53 (21) (2014) 4669–4674.
[22] X. Chen, K. Zhou, L. Zhang, I. Bennion, Dual-peak long-period fiber gratings with enhanced refractive index sensitivity by finely tailored mode dispersion that uses the light cladding etching technique, Appl. Opt. 46 (4) (2007) 451–455.
[23] Y. Liu, B. Liu, X. Feng, W. Zhang, G. Zhou, S. Yuan, G. Kai, X. Dong, High-birefringence fiber loop mirrors and their applications as sensors, Appl. Opt. 44 (12) (2005) 2382–2390.